ARTICLE

IMMUNOTHERAPY

Antibody blockade of the PSGL-1 immune checkpoint enhances T-cell responses to B-cell lymphoma

João L. Pereira[1,2,3], Liliana Arede[1], Francisca Ferreira[1,2,4], Andreia Matos[1,5,6,7,8], Dulcineia Pereira[1,2,9], Rita F. Santos[1,10,11], Alexandre M. Carmo[1,10], Maria J. Oliveira[1,3,5], José C. Machado[1,2,3], Delfim Duarte[1,3,9] and Nuno R. dos Santos[1,2]✉

Despite advancements in cancer immunotherapy, most lymphomas remain unresponsive to checkpoint inhibitors. P-selectin glycoprotein ligand-1 (PSGL-1), recently identified as a promoter of T-cell exhaustion in murine melanoma models, has emerged as a novel immune checkpoint protein and promising immunotherapeutic target. In this study, we investigated the potential of PSGL-1 antibody targeting in B-cell lymphoma. Using allogeneic co-culture systems, we demonstrated that targeted antibody interventions against human PSGL-1 enhanced T-cell activation and effector cytokine production in response to lymphoma cells. Moreover, in vitro treatment of primary lymphoma cell suspensions with PSGL-1 antibody resulted in increased activation of autologous lymphoma-infiltrating T cells. Using the A20 syngeneic B-cell lymphoma mouse model, we found that PSGL-1 antibody treatment significantly slowed tumor development and reduced the endpoint tumor burden. This antitumoral effect was accompanied by augmented tumor infiltration of $CD4^+$ and $CD8^+$ T cells and reduced infiltration of regulatory T cells. Finally, anti-PSGL-1 administration enhanced the expansion of CAR T cells previously transferred to mice bearing the aggressive Eμ-*Myc* lymphoma cells and improved disease control. These results demonstrate that PSGL-1 antibody blockade bolsters T-cell activity against B-cell lymphoma, suggesting a potential novel immunotherapeutic approach for treating these malignancies.

Leukemia (2025) 39:178–188; https://doi.org/10.1038/s41375-024-02446-w

INTRODUCTION

Lymphomas are generally classified as Hodgkin (~10% of cases) or non-Hodgkin lymphomas (NHLs, ~90% of cases), with NHL comprising several subtypes of B-cell (85–90%) and T-cell (10–15%) lymphomas [1, 2]. Although treatment options for B-cell lymphomas are generally based on chemotherapy cycles and, in specific cases, radiotherapy [1–3], other strategies such as immunotherapy (e.g., rituximab and brentuximab vedotin), stem cell transplantation and chimeric antigen receptor (CAR) T-cell therapy have also been applied in clinical practice [2, 4, 5]. The advent of immune checkpoint blockade therapies has led to high response rates in patients with lymphoma subtypes characterized by an inflamed microenvironment and frequent expression of programmed-cell death protein 1 (PD-1) ligands, such as Hodgkin lymphoma and primary mediastinal large B-cell lymphoma [2, 4, 6, 7]. Clinical trials have demonstrated particularly high response rates to the nivolumab and pembrolizumab PD-1 inhibitors in patients with relapsed or refractory Hodgkin lymphoma [5, 8, 9]. However, for most NHL subtypes, patients often show reduced response rates to immune checkpoint blockade therapies [5, 9, 10], likely because most of these malignancies are noninflamed and exhibit low PD-1 ligand expression [5, 7, 11, 12].

The P-selectin glycoprotein ligand-1 (PSGL-1), encoded by the *SELPLG* gene, has recently been identified as an immune response modulatory protein. Since it was first described in neutrophils as a ligand for P-selectin, PSGL-1 has been shown to interact with all selectin adhesion molecules (P-, E- and L- selectin) and to be associated with lymphoid and myeloid cell adhesion, migration and motility [13–20]. Furthermore, PSGL-1 has been reported to negatively regulate T-cell function. In fact, PSGL-1-deficient T cells from *Selplg* knockout (KO) mice exhibited enhanced proliferation compared to wild-type T cells following either TCR stimulation or homeostatic cytokine stimulation [21, 22]. More recently, PSGL-1 was shown to function as an immune checkpoint regulator by promoting mouse T-cell exhaustion, a dysfunctional state linked to

[1]i3S—Instituto de Investigação e Inovação em Saúde, Universidade do Porto, Porto, Portugal. [2]IPATIMUP—Institute of Molecular Pathology and Immunology, University of Porto, Porto, Portugal. [3]Faculty of Medicine, University of Porto, Porto, Portugal. [4]Master´s Program in Bioengineering, ICBAS—Instituto de Ciências Biomédicas Abel Salazar, and Faculty of Engineering, University of Porto, Porto, Portugal. [5]INEB—Instituto de Engenharia Biomédica, Universidade do Porto, Porto, Portugal. [6]ICBAS—Instituto de Ciências Biomédicas Abel Salazar, Universidade do Porto, Porto, Portugal. [7]Genetics Laboratory, Faculty of Medicine, University of Lisbon, Lisboa, Portugal. [8]Ecogenetics and Human Health, Environmental Health Institute, Faculty of Medicine, University of Lisbon, Lisboa, Portugal. [9]Department of Hematology and Bone Marrow Transplantation, IPO Porto, Porto, Portugal. [10]IBMC—Instituto de Biologia Molecular e Celular, Universidade do Porto, Porto, Portugal. [11]ESS—IPP, School of Health, Polytechnic of Porto, Porto, Portugal.
✉email: nunos@i3s.up.pt

Received: 5 March 2024 Revised: 12 October 2024 Accepted: 17 October 2024
Published online: 25 October 2024

persistent antigenic stimulation in inflammatory contexts [23], and restricting effector T-cell responses and memory T-cell development upon viral or tumoral challenges [24, 25]. Following viral infection, *Selplg*-deficient (*Selplg*$^{-/-}$) T cells exhibited enhanced survival, reduced expression of the inhibitory receptors PD-1, CD160, and BTLA, and increased production of effector cytokines [24, 25]. Moreover, *Selplg*$^{-/-}$ T cells responded more robustly to anti-PD-L1 treatment in vivo compared to wild-type T cells [26]. Similarly, anti-PD-1 therapy promoted tumor regression in melanoma-bearing *Selplg*$^{-/-}$ mice [27]. Furthermore, targeting PSGL-1 with a monoclonal antibody (mAb), either alone or in combination with PD-1 antibody blockade, enhanced effector CD4^{+} and CD8^{+} T-cell responses within tumors and reduced melanoma progression [27]. Beyond its role in regulating immune responses in T cells, recent evidence indicates that PSGL-1 also functions as an immunosuppressive checkpoint in tumor-associated macrophages [28].

Here, we addressed whether PSGL-1 blockade with specific antibodies could enhance T-cell activity against B-cell lymphoma. We show that in vitro treatment of human T cells with anti-PSGL-1 leads to increased T-cell activation in response to cocultured allogeneic lymphoma cells or autologous patient-derived lymphoma cells. Additionally, using B-cell lymphoma mouse models, we demonstrate the therapeutic potential of PSGL-1 blockade, either as a standalone treatment or in combination with CD19 CAR T-cell therapy.

MATERIALS AND METHODS

Generation of a PSGL-1-deficient Jurkat cell line

Three guide RNA (gRNA) sequences (#1, AATTACGCACGGGGTACAT; #2, GACAACTCGACTGACGGCCA; #3, TGGGGGAGTAATTACGCACGG) targeting the *SELPLG* second exon [29] were designed in the CRISPOR and Synthego software platforms [30] and selected for their high specificity, low off-target activity, high activity and early coding region. The gRNAs were inserted into the lentiCRISPR v2 plasmid, which was a gift from Feng Zhang (Addgene plasmid #52961; http://n2t.net/addgene:52961; RRID: Addgene_52961), after plasmid digestion with the *Esp*3I restriction enzyme (cat. no. ER0451, Thermo Scientific). To produce lentiviral particles, lentiCRISPR plasmids were transfected into HEK293T cells together with pRRE, pRev, and pMD2.G packaging plasmids, a gift from D. Trono (Addgene plasmids #12251, #12253, #12259), and pCEP4-tat, a gift from S. Kasparov (Addgene plasmid #22502), with Lipofectamine 2000 reagent (Invitrogen). After 72 h, collected supernatants were filtered through 0.22 µm filters (Whatman) and added immediately to 1×10^6 Jurkat cells growing in complete RPMI medium without antibiotics. Two days later, the transduced cells were selected by the addition of puromycin (0.5 µg/ml for two days and 1 µg/ml for two more days). The gRNA #2 showed increased efficacy in knocking out *SELPLG*, as verified by flow cytometry. Puromycin-resistant Jurkat cells infected with empty lentiCRISPR lentiviral particles (Jurkat/Mock) were obtained as controls. The Jurkat/*SELPLG* KO #2 PSGL-1-negative cells were isolated by flow cytometry sorting on a BD FACSAria II, and later cloned through serial dilution.

CAR T-cell generation

Anti-mouse CD19 CAR T cells were generated based on the Eremenko et al. [31] protocol. To confirm retroviral transduction and detect the CAR T construct, which is based on an IgG2aκ rat anti-CD19 antibody [32], in transduced T cells, we performed flow cytometry with Alexa Fluor 647-conjugated AffiniPure $F(ab')_2$ fragment mouse anti-rat IgG (cat. no. 212-606-168, Jackson ImmunoResearch).

Primary human T-cell isolation

Peripheral blood mononuclear cells (PBMCs) were obtained from buffy coats of healthy adult blood donors (aged 18–42 years; Table S1) provided by the local hospital blood bank (*Serviço de Imunohemoterapia, CHU São João, Porto)* after ethical approval (ref. no. 398/2020). PBMCs were isolated by density-gradient separation using Ficoll Paque Plus (Cytiva). The cell pellet was cleared of the remaining erythrocytes by incubation in red blood cell lysis buffer (144 mM NH_4Cl, 17 mM Tris-HCl) for 5 min at 37 °C, and then washed in phosphate-buffered saline. T cells were isolated using the MojoSort Human CD3 T-Cell Isolation Kit (cat. no. 480021, Biolegend) and EasySep Magnet (cat. no. 18000, StemCell Technologies) according to the manufacturer's instructions.

Primary human lymphoma samples

Lymph node biopsies collected between 2019 and 2023 from six B-cell lymphoma patients (Table S2) were obtained at the Onco-Hematology Department of IPO-Porto after informed consent and ethical approval (ref. GOM_PI_2013.03). This research was conducted according to the principles of the Declaration of Helsinki. Lymph node biopsies were processed by cutting small pieces with a scalpel in RPMI 1640 medium and dissociated by gentle pressure against a 0.75 µm cell strainer. For autologous co-culture experiments, lymph node suspensions were cultured in complete RPMI medium, with or without PL1 antibody (concentration of ~5–10 µg/ml) or mouse IgG (10 µg/ml, Jackson ImmunoResearch).

Subcutaneous A20 lymphoma mouse model

Mouse experimental procedures were approved by the i3S ethics committee (approval no. 15/CECRI/2020) and Portuguese authorities (*Direção-Geral de Agricultura e Veterinária*) and followed ethical guidelines (Directive 2010/63/EU and decree laws no. 113/2013 and 1/2019). 5×10^6 A20 cells were injected s.c. into BALB/c mice with 9 to 11 weeks of age. It was estimated that five mice per group would be sufficient to detect significant differences. No animals were excluded from analysis. When tumors became palpable in all mice, i.e., 7 days post-cell injection (dpi), mice were randomized to receive 200 µg of either PSGL-1 mAb (clone 4RA10, cat. no. BE0186, BioXcell) or control IgG (ChromPure rat IgG, cat. no. 012-000-003, Jackson ImmunoResearch). Mice were treated i.p. at 7, 10, and 13 dpi (in the late afternoon). Tumors were measured with calipers and tumor volume (*V*) was calculated using the formula: $V\ (mm^3) = (L \times W^2)/2$, where *L* is the largest and *W* is the smallest of two perpendicular tumor axes. No blinding analysis was done. Mice were euthanized by CO_2 inhalation at 20 dpi. At the experimental endpoint, mouse spleen and tumor cells were mechanically dissociated through a 70 µm cell strainer (cat. no. 352350, Falcon).

Eμ-*Myc* lymphoma mouse model

5×10^5 of Eμ-*Myc* green fluorescent protein-positive (GFP^{+}) lymphoma cells were injected intravenously (i.v.) into C57BL/6 J female mice. Percentage of GFP^{+} lymphoma cells in the blood was assessed by flow cytometry. Mice were randomly subdivided in two groups and then received i.p. 200 µg of either 4RA10 or control IgG at 6, 9, and 12 dpi before euthanasia at 13 dpi. For the CAR T-cell experimental setup, C57BL/6 J female mice were irradiated with 4 Gy, 4 h before the infusion of 5×10^5 Eμ-*Myc* GFP^{+} lymphoma cells. At 6 dpi, mice were infused i.v. with 6×10^6 CAR T cells. At 7, 9, and 11 dpi, mice randomly assigned to two groups were treated with 200 µg of either 4RA10 mAb or IgG control antibody, before euthanasia at 13 dpi. The mouse spleens, bone marrow, and lymph nodes were collected for flow cytometry analysis.

Statistics

Data plots were generated and statistical analyses were performed with GraphPad Prism software. Statistical tests and sample numbers are indicated in figure legends. Paired *t* tests were performed to compare stimulated versus unstimulated T cells and anti-PSGL-1-treated versus untreated T cells from healthy donors. Unpaired *t* tests were performed to compare tumor volumes, weights, and cell percentages between anti-PSGL-1-treated and control-treated mice. Simple linear regression was used to assess if the ratios of effector to naive T cells were correlated with tumor weight. A *P* value below 0.05 was considered statistically significant.

Additional materials and methods are reported in the Supplementary Information.

RESULTS

PSGL-1 genetic inactivation enhances T-cell receptor (TCR)-mediated human T-cell activation

To assess the impact of PSGL-1 genetic inactivation on human T-cell activation, we inactivated the *SELPLG* gene through CRISPR-Cas9 in the human Jurkat T-cell line (Figs. 1A and S1A), which is a well-established cellular model for studying the regulation of TCR signaling [33]. Next, we stimulated Jurkat/*SELPLG* KO and Jurkat/Mock cells with different concentrations of plate-bound anti-CD3

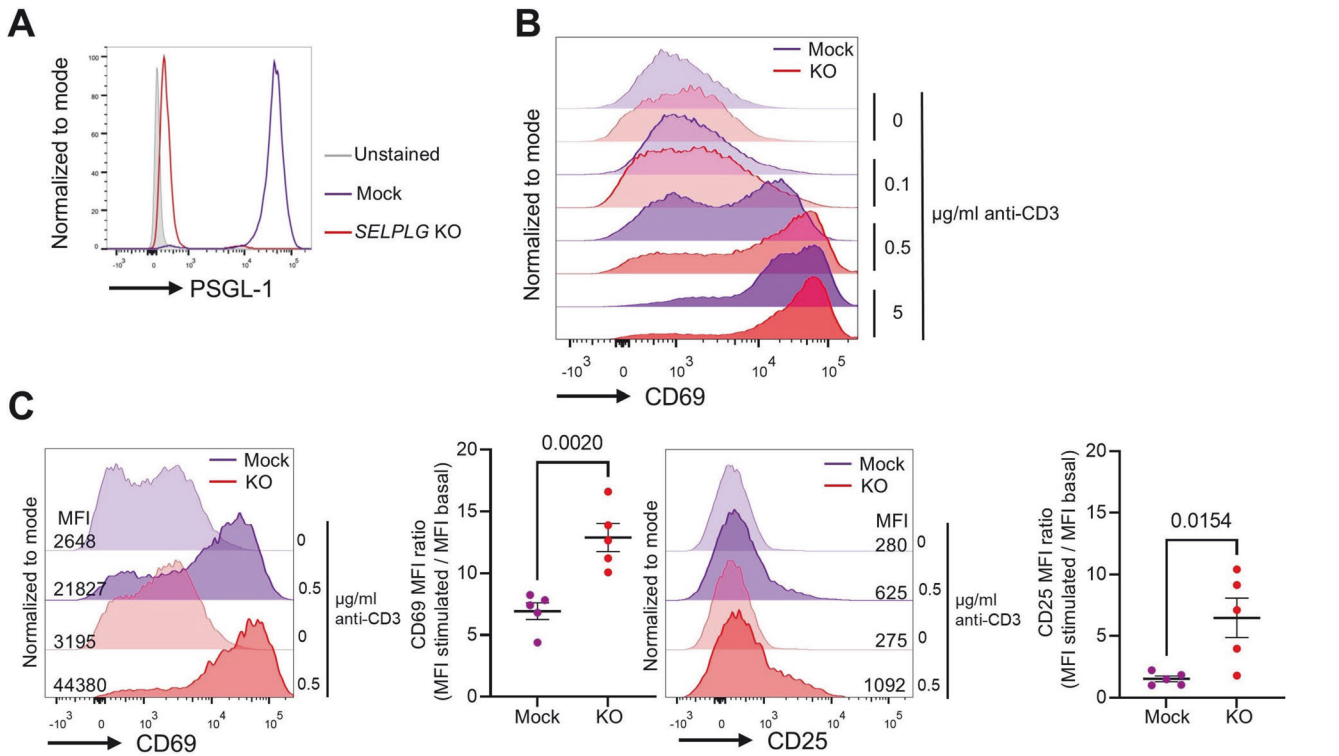

Fig. 1 PSGL-1 genetic inactivation enhances TCR/CD3-mediated T-cell activation. A Flow cytometry detection of PSGL-1 surface expression in Jurkat/Mock and Jurkat/*SELPLG* knockout (KO) cells. Unstained Jurkat/Mock cells are shown as a negative control. **B** CD69 surface expression levels of Jurkat/Mock and *SELPLG* KO cells after 24 h of anti-CD3 stimulation (basal levels and 0.1, 0.5, and 5 µg/ml of anti-CD3). Data are representative of two independent experiments. **C** Histograms and mean fluorescence intensity (MFI) ratio between CD3-stimulated (0.5 µg/ml, 24 h) and unstimulated Jurkat/Mock and *SELPLG* KO cells. Five independent CD3 stimulation experiments are represented in the graphs. *P* values obtained from unpaired *t* tests are shown.

and assessed T-cell activation by detecting the CD69 activation marker. Compared with Jurkat/Mock cells, Jurkat/*SELPLG* KO cells stimulated with low anti-CD3 concentrations had increased levels of CD69 (Fig. 1B). By stimulating Jurkat/Mock and *SELPLG* KO cells with 0.5 µg/ml anti-CD3, we found that CD25 was upregulated along with CD69 in Jurkat/*SELPLG* KO cells compared to Jurkat/Mock cells (Fig. 1C). Similar results were obtained upon CD3 stimulation of a clonal Jurkat/*SELPLG* KO cell line compared to Jurkat parental cells (Fig. S1B). In contrast to recent findings indicating that PSGL-1 negatively regulates the TCR signaling pathway in mouse T cells [34], our experiments did not reveal significant differences in ZAP-70 or ERK phosphorylation in Jurkat/*SELPLG* KO cells stimulated with anti-CD3 (Fig. S2). Nevertheless, our findings indicate that PSGL-1 deficiency renders Jurkat T cells more sensitive to weaker TCR/CD3 stimulation, and thus show that, as in mice, PSGL-1 is a regulator of human T-cell responses to antigenic stimulation.

Antibody blockade of PSGL-1 enhances TCR-induced T-cell activation

We next assessed whether blocking PSGL-1 with antibodies could produce a similar outcome as genetic deficiency. By coculturing Jurkat cells with Raji lymphoma cells pre-loaded with the staphylococcal enterotoxin B superantigen in the presence or absence of the anti-PSGL-1 PL1 mAb, which is known to inhibit PSGL-1 activity by blocking its interactions with selectins [15], we found that the levels of CD69 on Jurkat cells increased upon PL1 treatment (Fig. S3). We next addressed the effect of the PL1 mAb on the proliferation of normal human T cells. Notably, PL1 treatment modestly but significantly enhanced proliferation induced by CD3 stimulation (Fig. S4A).

We observed that PSGL-1 surface expression in Jurkat cells, detected by KPL-1 antibody—which recognizes a distinct epitope from PL1 [35]—decreased upon activation, with a more pronounced reduction following PL1 treatment (Fig. S3). These observations were matched in normal T cells, with both surface and overall PSGL-1 expression decreased following CD3/CD28 stimulation (Fig. S4B). Moreover, similar mean fluorescence levels in permeabilized and nonpermeabilized cells indicated that most PSGL-1 expression was localized on the surface of T cells (Fig. S4B). Although the PSGL-1 levels were higher in $CD8^+$ than in $CD4^+$ T cells, both populations exhibited decreased expression following activation (Fig. S4C, D).

Antibody blockade of PSGL-1 enhances T-cell activation in response to lymphoma cells

We cocultured healthy donor human T cells with allogenic Raji antigen-presenting cells, in the presence or absence of PL1 mAb. To facilitate the activation of a polyclonal population of unrelated donor T cells in response to Raji cells, the former were preactivated with CD3 and CD28 antibodies for 24 h (Fig. 2A). As expected, this led to CD25 and CD69 upregulation (Fig. S5A). Next, preactivated T cells were cultured with irradiated Raji lymphoma cells in the presence or absence of PL1 for 3, 5, or 7 days (Fig. 2A). Consistent with the observations in Jurkat cocultures (Fig. S3), PSGL-1 surface expression on $CD4^+$ and $CD8^+$ T cells decreased after 3 days of coculture with PL1 treatment (Fig. S5B). At all co-culture timepoints analyzed, the percentage of $CD69^+CD25^+$ activated T cells (gating strategy depicted in Fig. S5C) increased in the presence of PL1 compared to that in the absence of antibody (Fig. 2B–D), or with an IgG control (Fig. S5D). The activation-promoting effects of the PL1 antibody

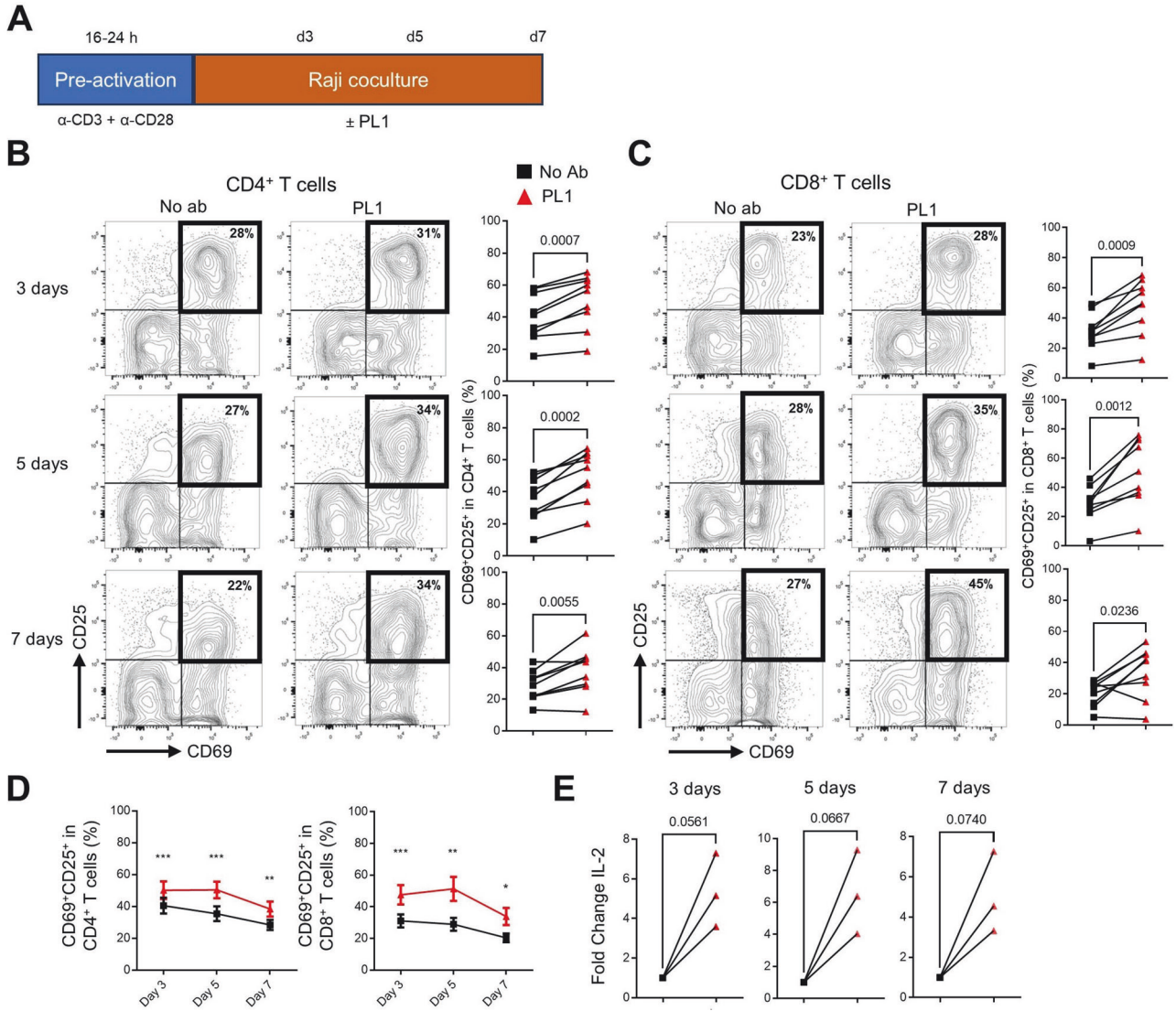

Fig. 2 Anti-PSGL-1 enhances T-cell activation in response to Raji lymphoma cells. A Schematic overview of the preactivated T-cell co-culture system with irradiated Raji lymphoma cells cultured for the indicated number of days (d). Representative flow cytometry dot plots showing the expression of CD25 and CD69 activation markers, highlighting the percentages of $CD4^+$-gated (**B**) and $CD8^+$-gated (**C**) $CD69^+CD25^+$ double-positive T cells after 3, 5, or 7 days of coculture with PL1 or no antibody (No Ab). The right plots show data from 9 independent healthy donors. **D** Percentage of $CD69^+CD25^+$ $CD4^+$ and $CD8^+$ healthy donor T cells after coculture with irradiated Raji lymphoma cells, with or without PL1 antibody. The data represent the mean ± standard error of the mean. **E** Fold-change differences in IL-2 production determined by ELISA between untreated and PL1-treated cocultures with T cells from three healthy donors. All *P* values were determined by paired *t* tests. * < 0.05, ** < 0.01, *** < 0.001.

on $CD4^+$ and $CD8^+$ T cells were most consistent at days 3 and 5 of coculture (Fig. 2B–D). Additionally, interleukin (IL)-2 secretion in the supernatant of $CD3^+$ T cells cocultured with Raji cells increased with PL1 treatment (Figs. 2E and S5E). These results demonstrate that the PSGL-1 antibody enhances T-cell activation in response to Raji lymphoma cells.

We next investigated the impact of PSGL-1 on human T cells primed to recognize lymphoma antigens. Healthy donor T cells were first stimulated with cocultured irradiated Raji lymphoma cells for 7 days, resulting in the upregulation of CD69, CD25, or both activation markers in an average of 27% of the T cells (Fig. S5F). Subsequently, the Raji-primed T cells were rechallenged with irradiated Raji cells, either with or without PL1, for an additional 5 days (Fig. 3A), which further induced CD25 and CD69 upregulation (Fig. 3B). Despite variability among individual donor samples, PSGL-1 antibody blockade consistently led to a higher percentage of $CD69^+$ and/or $CD25^+$ T cells compared to the control without antibody (Fig. 3B). These findings show that PSGL-1 antibody blockade enhances tumor antigen-mediated activation of lymphoma-primed T cells.

Antibody blockade of PSGL-1 enhances in vitro exhausted-like $CD4^+$ T-cell response to lymphoma cells

In tumors, persistent antigenic stimulation of infiltrating T cells often leads to a hyporesponsive state, commonly defined as exhaustion [23]. Thus, we assessed whether PSGL-1 antibody blockade could enhance the responses of exhausted T cells to lymphoma antigens. Chronic in vitro activation of healthy donor human T cells by continuously stimulating them with CD3/CD28 antibodies for 9 days (Fig. 4A) resulted in increased expression of the PD-1, LAG-3, and TIM-3 exhaustion markers in $CD4^+$ and $CD8^+$ T cells (Fig. S6A). To assess how exhausted-like T cells respond to lymphoma antigens with or without PSGL-1 blockade, they were cocultured with irradiated Raji cells for an additional

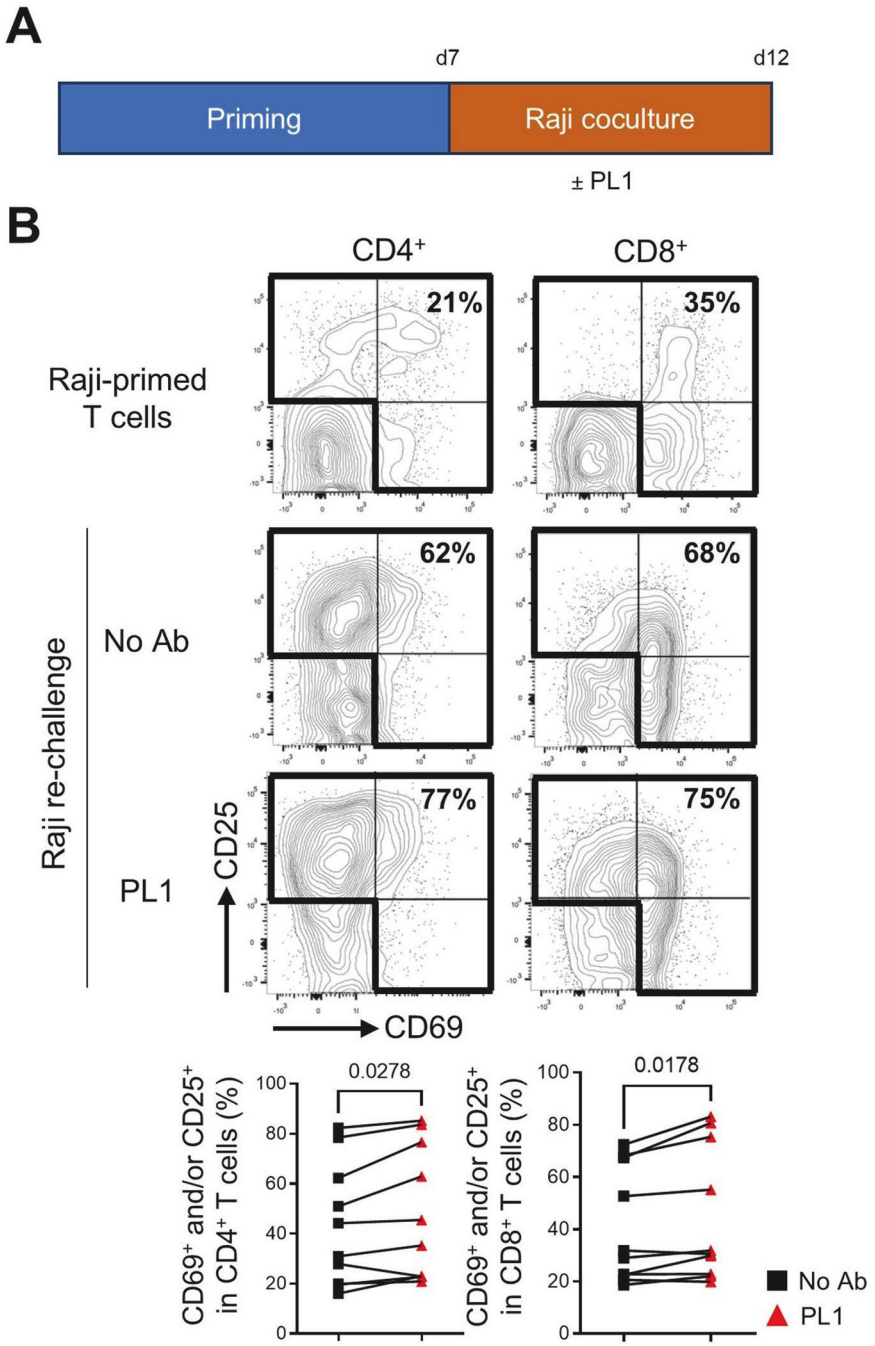

Fig. 3 Anti-PSGL-1 enhances primed T-cell activation in response to Raji lymphoma cells. A Schematic overview of the generation of primed T cells and co-culture settings with irradiated Raji lymphoma cells. **B** Representative flow cytometry dot plots and percentages of $CD4^+$-gated and $CD8^+$-gated healthy donor T cells positive for CD69 and/or CD25 after Raji cell rechallenge in the presence of PL1 mAb or absence of antibody (No Ab). The indicated *P* values were obtained from paired *t* tests. The bottom plots show data from 10 independent healthy donors.

5 days, either in the presence or absence of PL1 antibody (Fig. 4A), or cultured alone for 5 days as a control. Remarkably, the expression of CD69, at day 14, in $CD4^+$ but not $CD8^+$ T cells was enhanced when PL1 was present in cocultures (Fig. 4B). No significant changes in CD25 expression were observed (data not shown). Also, no statistically significant differences in PD-1, LAG-3, or TIM-3 expression were observed between Raji-cocultured T cells treated with PL1 and those not treated with PL1 (Fig. S6B), which suggested that PSGL-1 blockade did not promote $CD4^+$ T-cell activation through the downregulation of inhibitory receptors. We also assessed IL-2 and interferon (IFN)-γ cytokine production in the cocultures. Despite extensive variability across samples (Fig. S6C), PL1 treatment resulted in a statistically significant increase in IL-2 and IFN-γ production after value normalization (Fig. 4C). Together, these results suggest that PSGL-1 blockade enhances the activation and effector function of exhausted $CD4^+$ T cells in response to allogeneic lymphoma cells.

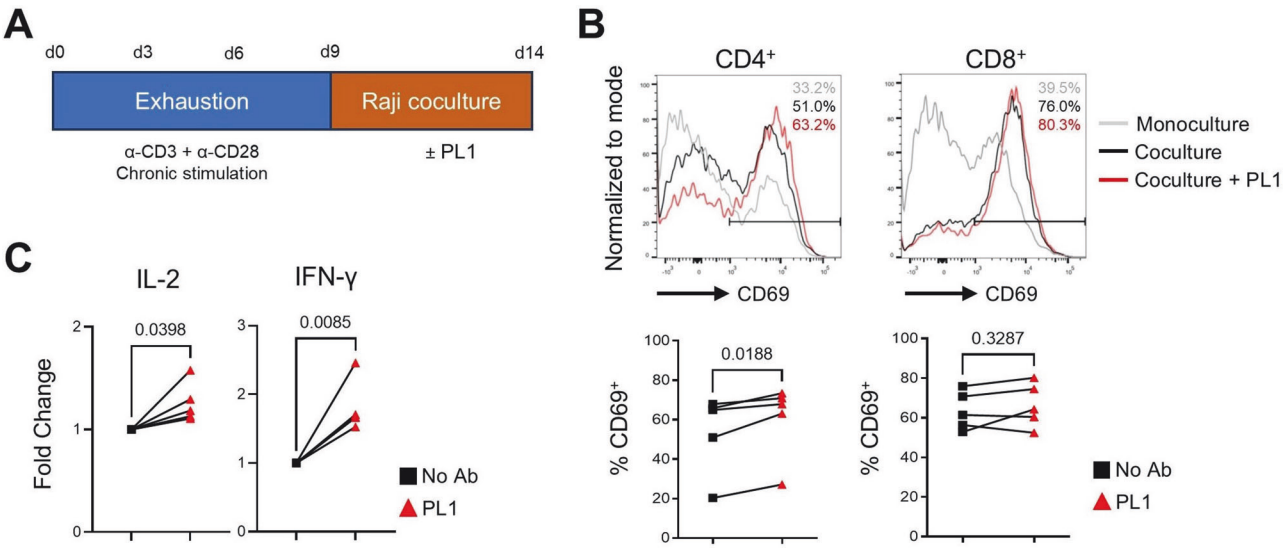

Fig. 4 Anti-PSGL-1 enhances exhausted-like CD4$^+$ T-cell response to Raji lymphoma cells. A Schematic overview of the induction of T-cell exhaustion in healthy donor T cells for 9 days (d) followed by 5 days of coculture with irradiated Raji lymphoma cells. **B** Representative flow cytometry histograms showing the percentage of CD4$^+$- and CD8$^+$-gated T cells expressing CD69 on day 5 of coculture. As a control, the percentage of exhausted-like T cells expressing CD69 after culture alone for further 5 days and without any stimulation (Monoculture) is shown. The bottom plots show data from 5 independent healthy donors. The indicated *P* values were obtained from paired *t* tests. **C** Fold-change differences in IL-2 and IFN-γ production determined by ELISA between no antibody and PL1-treated cocultures with T cells from five healthy donors. All *P* values were determined by paired *t* tests.

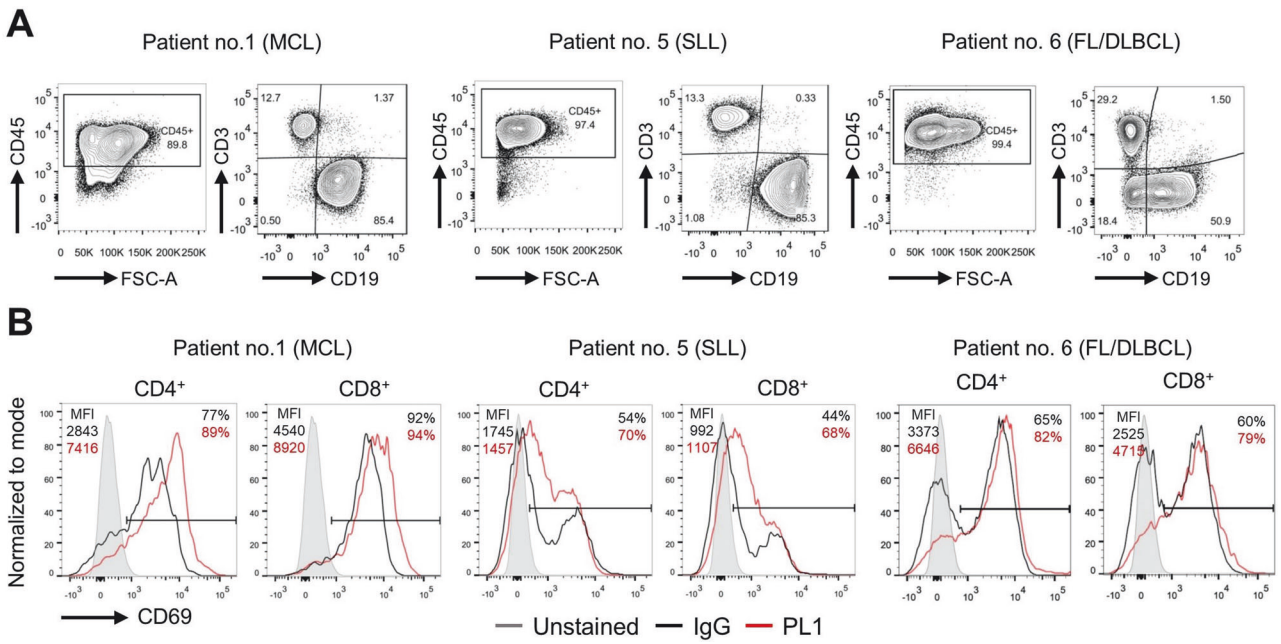

Fig. 5 PSGL-1 antibody blockade enhances lymphoma patient T-cell activation. A Flow cytometry characterization of T (CD3$^+$) and B (CD19$^+$) lineage populations within gated CD45$^+$ cells from lymph node (LN) biopsies of three B-cell lymphoma patients from the indicated subtypes. **B** Flow cytometry detection and MFI of CD69 surface expression in LN-derived CD4$^+$ and CD8$^+$ T cells after 3 days of culture with IgG or PL1 antibodies. MCL mantle cell lymphoma, SLL small lymphocytic lymphoma, FL/DLBCL diffuse large B-cell lymphoma transformed from a follicular lymphoma.

Antibody blockade of PSGL-1 enhances the activation of patient lymphoma-infiltrating T cells

To assess whether PSGL-1 antibody blockade can enhance human T-cell activation in response to autologous lymphoma antigens, patient-derived lymphoma cells were cocultured with their respective infiltrating T cells. Unsorted single-cell suspensions from lymph node biopsies of six B-cell lymphoma patients of different subtypes (one mantle cell lymphoma, one small lymphocytic lymphoma, one diffuse large B-cell lymphoma (DLBCL) transformed from a follicular lymphoma, and three DLBCLs), were cultured for 3 days with PL1 mAb, IgG or no antibody. The proportion of lymphoma and T cells in each biopsy ranged from ~40% to 80% and 10% to 50%, respectively, except for one DLBCL biopsy (patient no. 4), which exhibited a low percentage of lymphoma cells (Figs. 5A, S7A, S8). Furthermore, PSGL-1 expression was observed in both malignant B cells and

infiltrating T cells, with higher levels in the latter (Fig. S9). After 3 days of autologous coculture, $CD4^+$ and $CD8^+$ T cells from three lymphoma patient samples exhibited higher CD69 expression with PL1 treatment compared to negative controls (Fig. 5B). In contrast, CD25 expression in T cells was not significantly altered by PL1 treatment (data not shown). For three DLBCL biopsies, PL1 treatment had no significant impact on either CD69 or CD25 expression (Fig. S7B). We hypothesized that the acquisition of an exhaustion phenotype might predict a lack of responsiveness to PSGL-1 blockade. However, all lymphoma samples expressed varying levels of exhaustion markers, with no clear correlation between their expression and the response to PL1 treatment (Fig. S7C). Additionally, PL1 treatment had no significant impact on exhaustion marker expression, except for an increased percentage of TIM-3-expressing T cells in PL1-responsive lymphoma cases (Fig. S7C). This indicates that PL1-mediated enhancement of T-cell activation did not depend on the down-regulation of inhibitory receptors. Overall, these findings support the notion that targeting PSGL-1 with an antibody enhances T-cell activation in response to human lymphoma antigens.

PSGL-1 in vivo blockade increases effector immune cell infiltration of tumors and reduces murine lymphoma burden

To demonstrate the in vivo potential of PSGL-1 targeting to enhance T-cell responses to lymphoma, we used a B-cell lymphoma mouse model based on the subcutaneous inoculation of the A20 cell line in syngeneic mice. T cells infiltrating A20 tumors expressed PSGL-1, with $CD8^+$ tumor-infiltrating and splenic T cells showing higher expression than $CD4^+$ counterparts (Fig. S10). At 7 dpi, when subcutaneous tumors were palpable, the recipient mice were treated with either anti-PSGL-1 4RA10 mAb or control IgG (Fig. 6A). Strikingly, tumor progression was significantly impaired by 4RA10 treatment (Figs. 6B and S11A), resulting in smaller tumors at the experimental endpoint than in the control group (Fig. 6C). What is more, for two mice the 4RA10 treatment induced regression of the emerging tumor (Fig. S11A). Although the A20 cell line also expresses surface PSGL-1 [36], 4RA10 did not induce A20 cell death in vitro (Fig. S11B), which argues against a direct effect of the antibody treatment on tumor cells. To determine whether the reduced tumor growth in anti-PSGL-1-treated mice was associated with an increased immune response, we characterized the tumor-infiltrating immune component by flow cytometry (Fig. S12). Interestingly, the proportions of both $CD4^+$ and $CD8^+$ T cells were significantly greater in tumors from 4RA10-treated mice than in tumors from IgG-treated mice (Fig. 6D). Furthermore, 4RA10-treated mice displayed greater tumor infiltration by macrophages, dendritic cells, and natural killer (NK) cells than did IgG-treated mice (Fig. 6E).

Characterization of tumor-infiltrating $CD4^+$ and $CD8^+$ T cells, revealed that, unlike splenic T cells from tumor-bearing or wild-type mice, most were effector memory (T_{EM}, $CD44^+CD62L^-$) or central memory (T_{CM}, $CD44^+CD62L^+$), with very few naive (T_N, $CD44^-CD62L^+$) T cells (Fig. S13A, B). This suggests that the tumor-infiltrating T cells had undergone prior antigenic stimulation. Although 4RA10 treatment did not significantly alter the differentiation profile of tumor-infiltrating (Fig. S13B) or splenic T cells (Fig. S13C), we found that $CD4^+$ and $CD8^+$ T cells infiltrating smaller tumors (under 500 mg) displayed a higher T_{EM}/T_N ratio than those infiltrating larger ones (Fig. 6F). This suggests that T_{EM} cells underlie the decreased tumor burden verified in some 4RA10-treated mice. In line with the notion that PSGL-1 regulates T-cell activation, the proportion of tumor-infiltrating $CD8^+$ T cells expressing the CD69, CD25, and PD-1 activation markers was higher in tumors from 4RA10-treated mice than in those from IgG-treated mice (Fig. 6G). This effect of the 4RA10 treatment was restricted to $CD8^+$ T cells since no major differences in the expression of activation markers were observed for tumor-infiltrating $CD4^+$ T cells (Fig. S14A). Notably, $CD8^+$ T cells from the spleens of 4RA10-treated tumor-bearing mice also expressed more frequently CD69 and CD25 compared to those from IgG-treated mice (Fig. S14B) suggesting that the 4RA10 treatment also exerted systemic effects. Finally, although the frequency of $CD4^+$ $Foxp3^+$ regulatory T cells (Tregs) in the spleens of tumor-bearing mice was not significantly impacted by 4RA10 treatment (Fig. S14C), the percentage of Tregs infiltrating 4RA10-treated tumors was lower than that infiltrating IgG-treated tumors (Fig. 6H). These results show that PSGL-1 blockade increases tumor infiltration by activated $CD8^+$ T cells while decreasing Treg infiltration, likely contributing to the impaired tumor progression in anti-PSGL-1-treated mice.

Anti-PSGL-1 enhances CAR T-cell expansion and lymphoma burden control

We explored the therapeutic potential of PSGL-1 antibody blockade in a different lymphoma mouse model, based on the i.v. infusion of GFP-tagged Eμ-*Myc* lymphoma cells into syngeneic mice. Upon leukemia emergence, mice were then treated with either control IgG or 4RA10 mAb (Fig. S15A). Leukemia progressed rapidly in the blood with no significant differences between IgG- and 4RA10-treated mice (Fig. S15A, B). At the experimental endpoint, 4RA10-treated mice showed a lower percentage of GFP^+ lymphoma cells and reduced lymphocyte counts in the blood compared to IgG-treated mice (Fig. S15A–C), but these differences did not reach statistical significance. Although 4RA10 treatment did not impact lymphoma cell infiltration in the spleen and lymph nodes (Fig. S15D), spleens of 4RA10-treated mice showed a significantly increased pool of $CD8^+$ T_{CM} cells compared to IgG-treated mice (Fig. S15E), indicating that 4RA10 promoted T-cell differentiation. Overall, these results show that anti-PSGL-1 treatment alone was not effective in combating the aggressive Eμ-*Myc* lymphoma model.

To assess whether combining anti-PSGL-1 with other therapeutic strategies could enhance T-cell responses and improve lymphoma control, we investigated the combination of CAR T-cell therapy with 4RA10 mAb administration. CAR T cells targeting the CD19 B-cell marker were generated and infused into immunocompetent mice previously injected with GFP^+ Eμ-*Myc* lymphoma cells (Fig. 7A). Compared to untreated lymphoma-bearing mice, those infused with CAR T cells exhibited a reduced lymphoma burden in the peripheral blood and lymph nodes at experimental endpoint (Fig. 7B). Importantly, 4RA10-treated mice showed an even greater reduction in the percentage of lymphoma cells in the peripheral blood and lymph nodes (Fig. 7B). Strikingly, mice treated with anti-PSGL-1 consistently exhibited higher percentages of CAR T cells in the blood, bone marrow, and lymph nodes compared to IgG-treated mice (Fig. 7B). Moreover, CAR T cells in the lymph nodes, but not in the spleen, of 4RA10-treated mice showed a higher percentage and increased levels of the CD69 activation marker compared to those in IgG-treated mice (Fig. S16A). This observation, along with the fact that the CD19 CAR T cells express high levels of PSGL-1 (Fig. S16B), suggests that CAR T-cell expansion following PSGL-1 blockade is associated with increased TCR activation. These results demonstrate that CAR T therapy synergizes with anti-PSGL-1, resulting in both the expansion of CAR T cells and increased lymphoma control in a model where anti-PSGL-1 alone was insufficient to hinder disease progression.

DISCUSSION

In line with the function of PSGL-1 as an immune checkpoint protein in T cells, we demonstrate here the potential of PSGL-1 antibody targeting in enhancing T-cell responses against lymphoma. Our findings indicate that this approach increases the recruitment of activated T cells to tumors, expands CAR T cells and reduces tumor growth.

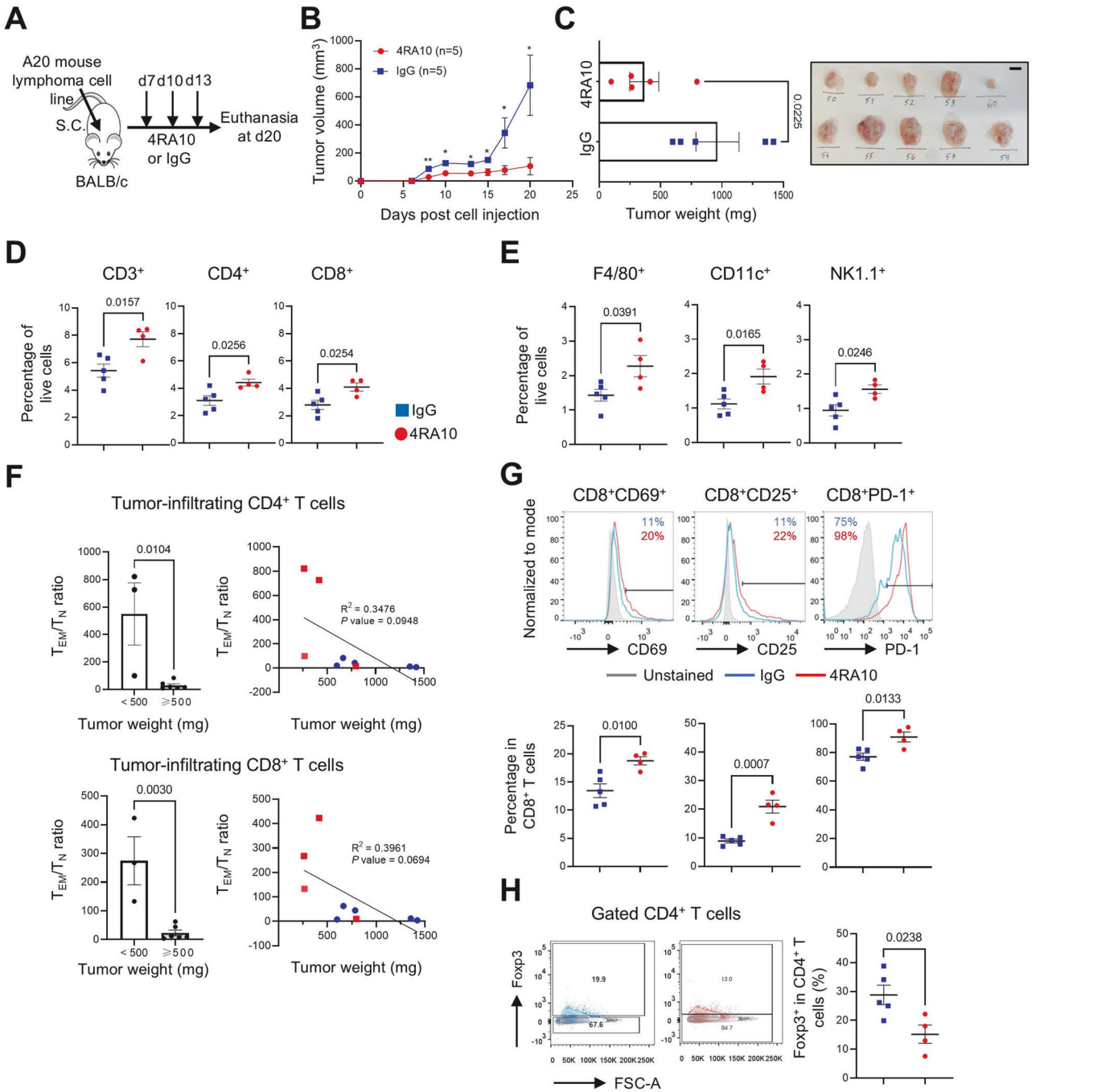

Fig. 6 In vivo administration of anti-PSGL-1 decreased lymphoma burden and increased tumor infiltration by activated T cells. **A** Schematic overview of the syngeneic lymphoma mouse model experimental protocol. **B** Tumor volume of rat IgG- and 4RA10-treated mice. The data points and error bars represent mean ± standard error of the mean (SEM) of IgG-treated and 4RA10-treated mice ($n = 5$ for each group). *$P < 0.05$, **$P < 0.01$; unpaired t tests. **C** Tumor weight ($n = 5$ for each group) and photograph of tumors on day 20. The columns and error bars represent mean ± SEM. **D** Percentages of tumor-infiltrating CD3$^+$, CD4$^+$, and CD8$^+$ T cells. **E** Percentages of tumor-infiltrating macrophages (F4/80$^+$), dendritic cells (CD11c$^+$), and NK cells (NK1.1$^+$). **F** Left plots, T_{EM}/T_N ratio of CD4$^+$ and CD8$^+$ tumor-infiltrating T cells in tumors subdivided according to weight. Right graphs, correlation between the T_{EM}/T_N ratio and tumor weight. The slope P value was obtained from simple linear regression test. **G** Upper panels, representative cytometry histograms showing expression of the CD69, CD25, and PD-1 activation markers in tumor-infiltrating CD8$^+$ T cells. Lower panels, percentage of tumor-infiltrating CD8$^+$ T cells expressing CD69, CD25, and PD-1. **H** Left panels, representative cytometry plots showing the percentage of Foxp3$^+$ tumor-infiltrating Tregs within the CD4$^+$ population. Right panel, percentage of tumor-infiltrating Tregs (CD4$^+$ Foxp3$^+$). For (**C**–**F** (left plots), **G**, **H**), the indicated P values were obtained by unpaired t tests. For (**D**–**H**), $n = 5$ for the IgG group (blue squares) and $n = 4$ for the 4RA10 group (red circles).

Treatment of A20 lymphoma-bearing mice with anti-PSGL-1 led to an increased percentage of tumor-infiltrating immune cells and enhanced the activation of both tumor-infiltrating and peripheral CD8$^+$ T cells. These findings parallel those reported for anti-PD-1-treated A20 lymphoma mice in that, like 4RA10, anti-PD-1 hampered tumor growth and increased CD69 expression levels in tumor-infiltrating CD8$^+$ T cells [37]. In addition, 4RA10 treatment of a syngeneic melanoma mouse model increased

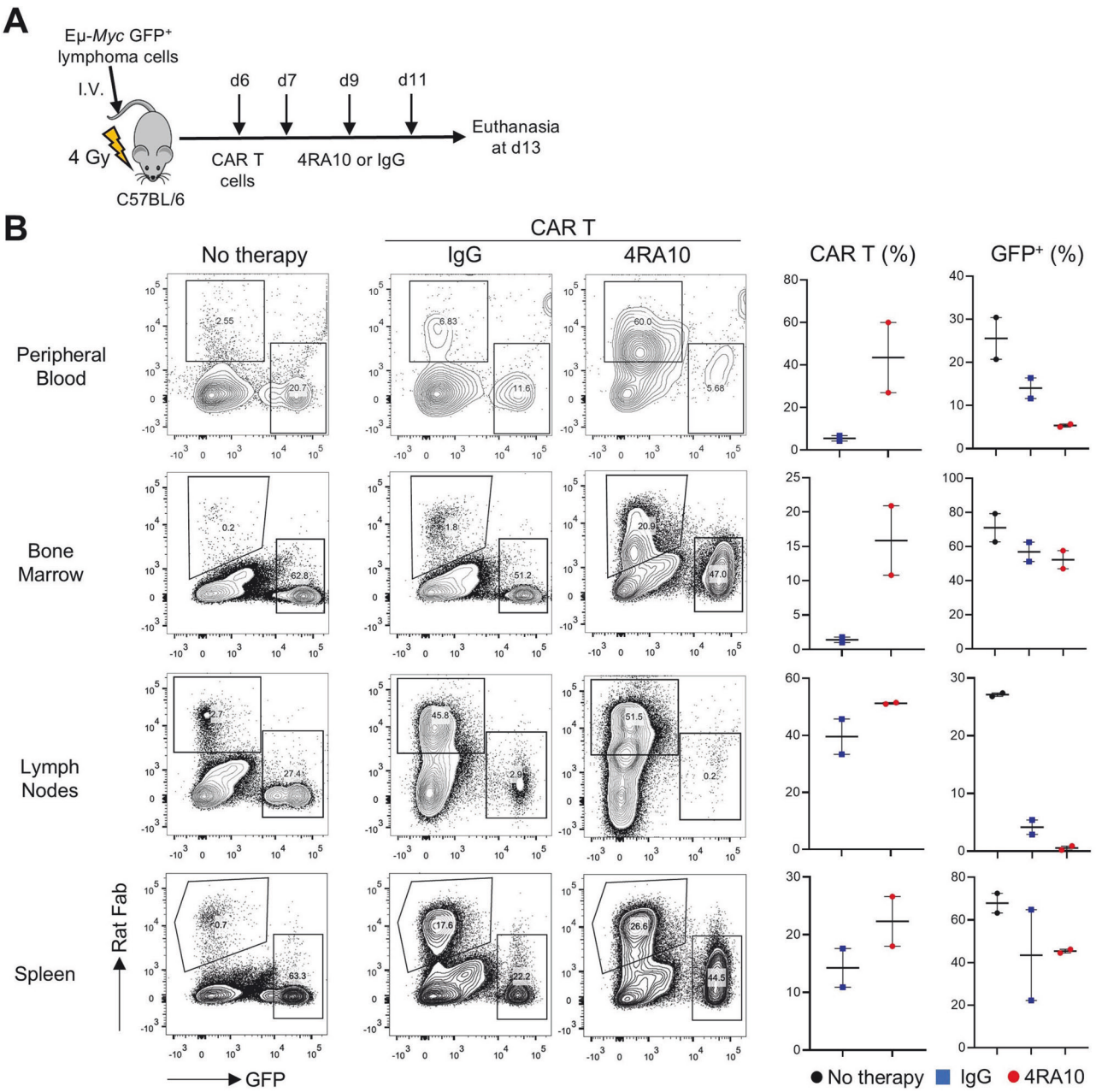

Fig. 7 Anti-PSGL-1 treatment increases CAR T-cell expansion in vivo and improves lymphoma burden control. A Schematic overview of the Eμ-*Myc* lymphoma mouse model treatment protocol. **B** Representative cytometry plots and graphs depicting the percentage of CAR T cells (positive for rat Fab) and lymphoma cells (positive for green fluorescent protein [GFP$^+$]) gated in live single cells from the peripheral blood, bone marrow, lymph nodes, and spleen of untreated mice (no therapy) and mice inoculated with CAR T cells at day 6 and treated with IgG or 4RA10 antibodies at days 7, 9, and 11.

antitumor T-cell responses, slowed tumor growth, increased the activation of CD4$^+$ and CD8$^+$ tumor-infiltrating T cells, and decreased Treg frequencies in tumors [27]. Notably, Hope et al. [34] reported that PSGL-1 blockade using recombinant soluble PSGL-1 protein also decreased tumor growth in a syngeneic melanoma model. Furthermore, it was reported that treatment of sarcoma, bladder, and colon syngeneic mouse models with anti-PSGL-1 resulted in decreased tumor growth, which could be further enhanced by combination therapy with an anti-PD-1 mAb [28]. Treatment of humanized mice bearing patient-derived melanoma xenografts with anti-PSGL-1 also resulted in decreased tumor growth [28]. Our work in lymphoma, together with previous research in melanoma and other cancers, shows that disrupting PSGL-1 interactions, either with specific antibodies or recombinant PSGL-1, results in increased antitumor immune activity and reduced tumor growth and that, similar to PD-1, PSGL-1 functions in T cells as a targetable immune checkpoint protein.

Unlike in the A20 lymphoma model, anti-PSGL-1 alone did not hamper lymphoma development in mice infused with Eμ-*Myc* malignant cells. As previously reported [38], CD19-targeted CAR T-cell treatment reduced lymphoma burden in mice, but co-administration of anti-PSGL-1 resulted in an even greater reduction of lymphoma burden in both lymphoid organs and peripheral blood. Strikingly, anti-PSGL-1 enhanced CAR T-cell expansion, suggesting that the improved lymphoma suppression induced by anti-PSGL-1 was primarily mediated through its direct

effect on CAR T cells. Although our results were based on a small number of mice, the effects of anti-PSGL-1 on CAR T-cell expansion and lymphoma burden were striking, suggesting that anti-PSGL-1 administration could synergize with CAR T cells to improve the treatment of aggressive lymphomas.

Using T cells from multiple healthy donors, we demonstrated that PSGL-1 antibody targeting enhanced their responses against lymphoma cells. The percentage of activated T cells in allogeneic cocultures—both with or without PSGL-1 blockade—varied remarkably among donor samples. This variability may be attributed to interindividual differences in HLA alleles, as well as factors such as sex and age, or recent exposure to antigenic challenges. Consistent with previous findings [39], PBMCs from different donors had different frequencies of T_N, T_{CM}, T_{EM} and terminally differentiated effector T cells (Fig. S17), potentially leading to variable responses to Raji lymphoma antigens. Despite this sample heterogeneity, our results support the notion that PSGL-1 is an inhibitory protein in human T cells, and that antibodies targeting the PSGL-1 extracellular domain can enhance antitumor T-cell responses, echoing previous reports on mouse PSGL-1 targeting [27]. Crucially, treatment of patient lymphoma-infiltrating T cells with PL1 resulted in increased activation of both $CD4^+$ and $CD8^+$ T cells in response to autologous lymphoma cells. Although this effect was noted in only three out of six patient samples, it highlights the potential of PSGL-1 antibodies for treating human lymphomas. The variability in response to anti-PSGL-1 therapy may depend on the specific B-cell lymphoma subtypes or the unique cellular and molecular features of lymphoma and T cells in each patient. Further studies are needed to validate these findings and identify which patients are most likely to benefit from this therapeutic approach.

Tumor-infiltrating T cells often exhibit an exhausted phenotype characterized by the expression of Eomes, Tcf-1, and Tox transcription factors; high expression of specific surface markers, such as PD-1, LAG-3, TIM-3, and CTLA-4; metabolic changes; and reduced T-cell effector function [23, 24, 26, 34]. PSGL-1 genetic inactivation was shown to promote effector functions in exhausted T cells either alone [34] or in combination with PD-1 blockade [26]. Here, we found that PSGL-1 blockade of in vitro-generated exhausted-like T cells significantly improved $CD4^+$ T-cell responses. These findings support the concept that PSGL-1 blockade could render exhausted T cells more active in antitumor responses. However, further studies should investigate whether combining PSGL-1 blockade with the blockade of other inhibitory receptors can more robustly promote the activation of exhausted human T cells.

At present, the molecular mechanisms by which PSGL-1 negatively regulates T-cell activation remain poorly defined. Our findings indicate that *SELPLG* deficiency renders human T cells more responsive to antigenic stimuli and confirms recent mouse knockout studies that uncovered the regulatory function of PSGL-1 in T-cell responses to viral or tumor antigens [24, 26, 27, 34]. Although *Selplg*-deficient mouse T cells exhibited increased levels of phosphorylated ERK, ZAP-70, and Akt kinases [34], we did not observe any significant differences in ERK and ZAP-70 activation upon CD3 stimulation of Jurkat cells, regardless of PSGL-1 expression. This suggests that PSGL-1 does not regulate the initiation of the TCR signaling pathway but may regulate downstream TCR-induced gene expression programs. Mechanistic studies are warranted to elucidate how PSGL-1 regulates human T-cell function.

In summary, our findings demonstrate that antibody blockade of PSGL-1 enhances T-cell activation in response to lymphoma cells. These results underscore the potential of targeting PSGL-1 as an immunotherapeutic strategy for treating this type of cancer. Additionally, our preliminary data suggest that anti-PSGL-1 therapy may enhance existing lymphoma treatments, including CAR T-cell therapy. We recently reported that the PL1 antibody could induce apoptosis in T and B lymphoma cell lines expressing PSGL-1 [40]. This cytotoxic effect was not universal because not all B-cell lymphoma cell lines were susceptible to PL1 targeting. Although in this report the A20 cell line and the six primary lymphoma cell samples did not undergo significant cell death upon incubation with anti-PSGL-1, our earlier and current findings indicate that targeting PSGL-1 could serve a dual purpose in lymphoma therapy: it may induce the apoptosis of lymphoma cells [40] while simultaneously enhancing the effector function of T cells.

DATA AVAILABILITY

The datasets generated during and/or analyzed during the current study are available from the corresponding author on reasonable request.

REFERENCES

1. Armitage JO, Gascoyne RD, Lunning MA, Cavalli F. Non-Hodgkin lymphoma. Lancet. 2017;390:298–310.
2. Ansell SM. Hodgkin lymphoma: 2018 update on diagnosis, risk-stratification, and management. Am J Hematol. 2018;93:704–15.
3. Michot JM, Lazarovici J, Ghez D, Danu A, Fermé C, Bigorgne A, et al. Challenges and perspectives in the immunotherapy of Hodgkin lymphoma. Eur J Cancer. 2017;85:67–77.
4. Lulla P, Heslop HE. Checkpoint inhibition and cellular immunotherapy in lymphoma. Hematol Am Soc Hematol Educ Program. 2016;2016:390–6.
5. Merryman RW, Armand P, Wright KT, Rodig SJ. Checkpoint blockade in Hodgkin and non-Hodgkin lymphoma. Blood Adv. 2017;1:2643–54.
6. Matsuki E, Younes A. Checkpoint inhibitors and other immune therapies for Hodgkin and non-Hodgkin lymphoma. Curr Treat Options Oncol. 2016;17:31.
7. Kline J, Godfrey J, Ansell SM. The immune landscape and response to immune checkpoint blockade therapy in lymphoma. Blood. 2020;135:523–33.
8. Tarekegn K, Ramosa AC, Singh B, Sequeira Grossa HG, Gupta S. Checkpoint Inhibitors in relapsed/refractory classical Hodgkin lymphoma. World J Oncol. 2021;12:51–4.
9. Xie W, Medeiros LJ, Li S, Yin CC, Khoury JD, Xu J. PD-1/PD-L1 pathway and its blockade in patients with classic Hodgkin lymphoma and non-Hodgkin large-cell lymphomas. Curr Hematol Malig Rep. 2020;15:372–81.
10. Perdikis-Prati S, Sheikh S, Bouroumeau A, Lang N. Efficacy of immune checkpoint blockade and biomarkers of response in lymphoma: a narrative review. Biomedicines. 2023;11:1720.
11. Hawkes EA, Grigg A, Chong G. Programmed cell death-1 inhibition in lymphoma. Lancet Oncol. 2015;16:e234–45.
12. Andorsky DJ, Yamada RE, Said J, Pinkus GS, Betting DJ, Timmerman JM. Programmed death ligand 1 is expressed by non-Hodgkin lymphomas and inhibits the activity of tumor-associated T cells. Clin Cancer Res. 2011;17:4232–44.
13. Moore KL, Stults NL, Diaz S, Smith DF, Cummings RD, Varki A, et al. Identification of a specific glycoprotein ligand for P-selectin (CD62) on myeloid cells. J Cell Biol. 1992;118:445–56.
14. Guyer DA, Moore KL, Lynam EB, Schammel CMG, Rogelj S, McEver RP, et al. P-selectin glycoprotein ligand-1 (PSGL-1) is a ligand for L-selectin in neutrophil aggregation. Blood. 1996;88:2415–21.
15. Moore KL, Patel KD, Bruehl RE, Fugang L, Johnson DA, Lichenstein HS, et al. P-selectin glycoprotein ligand-1 mediates rolling of human neutrophils on P-selectin. J Cell Biol. 1995;128:661–71.
16. Laszik Z, Jansen P, Cummings R, Tedder T, McEver R, Moore K. P-selectin glycoprotein ligand-1 is broadly expressed in cells of myeloid, lymphoid, and dendritic lineage and in some nonhematopoietic cells. Blood. 1996;88:3010–21.
17. Wilkins PP, Moore KL, McEver RP, Cummings RD. Tyrosine sulfation of P-selectin glycoprotein ligand-1 is required for high affinity binding to P-selectin. J Biol Chem. 1995;270:22677–80.
18. Walcheck B, Moore KL, McEver RP, Kishimoto TK. Neutrophil-neutrophil interactions under hydrodynamic shear stress involve L-selectin and PSGL-1: A mechanism that amplifies initial leukocyte accumulation on P-selectin in vitro. J Clin Invest. 1996;98:1081–7.
19. Borges E, Pendl G, Eytner R, Steegmaier M, Zöllner O, Vestweber D. The binding of T cell-expressed P-selectin glycoprotein ligand-1 to E- and P-selectin is differentially regulated. J Biol Chem. 1997;272:28786–92.
20. Martinez M, Joffraud M, Giraud S, Baïsse B, Bernimoulin MP, Schapira M, et al. Regulation of PSGL-1 interactions with L-selectin, P-selectin, and E-selectin: role of human fucosyltransferase-IV and -VII. J Biol Chem. 2005;280:5378–90.

21. Matsumoto M, Miyasaka M, Hirata T. P-selectin glycoprotein ligand-1 negatively regulates T-cell immune responses. J Immunol. 2009;183:7204–11.
22. Veerman KM, Carlow DA, Shanina I, Priatel JJ, Horwitz MS, Ziltener HJ. PSGL-1 regulates the migration and proliferation of CD8+ T cells under homeostatic conditions. J Immunol. 2012;188:1638–46.
23. McLane LM, Abdel-Hakeem MS, Wherry EJ. CD8 T cell exhaustion during chronic viral infection and cancer. Annu Rev Immunol. 2019;37:457–95.
24. Tinoco R, Carrette F, Barraza ML, Otero DC, Magaña J, Bosenberg MW, et al. PSGL-1 Is an immune checkpoint regulator that promotes T cell exhaustion. Immunity. 2016;44:1190–203.
25. Tinoco R, Neubert EN, Stairiker CJ, Henriquez ML, Bradley LM. PSGL-1 is a T cell intrinsic inhibitor that regulates effector and memory differentiation and responses during viral infection. Front Immunol. 2021;12:677824.
26. Viramontes KM, Neubert EN, DeRogatis JM, Tinoco R. PD-1 immune checkpoint blockade and PSGL-1 inhibition synergize to reinvigorate exhausted T cells. Front Immunol. 2022;13:869768.
27. DeRogatis JM, Viramontes KM, Neubert EN, Henriquez ML, Guerrero-Juarez CF, Tinoco R. Targeting the PSGL-1 immune checkpoint promotes immunity to PD-1–resistant melanoma. Cancer Immunol Res. 2022;10:612–25.
28. Kauffman K, Manfra D, Nowakowska D, Zafari M, Nguyen PA, Phennicie R, et al. PSGL-1 blockade induces classical activation of human tumor-associated macrophages. Cancer Res Commun. 2023;3:2182–94.
29. Yang J, Hirata T, Croce K, Merrill-Skoloff G, Tchernychev B, Williams E, et al. Targeted gene disruption demonstrates that P-selectin glycoprotein ligand 1 (PSGL-1) is required for P-selectin-mediated but not E-selectin-mediated neutrophil rolling and migration. J Exp Med. 1999;190:1769–82.
30. Concordet JP, Haeussler M. CRISPOR: intuitive guide selection for CRISPR/Cas9 genome editing experiments and screens. Nucleic Acids Res. 2018;46:W242–5.
31. Eremenko E, Taylor ZV, Khand B, Zaccai S, Porgador A, Monsonego A. An optimized protocol for the retroviral transduction of mouse CD4 T cells. STAR Protoc. 2021;2:100719.
32. Kochenderfer JN, Yu Z, Frasheri D, Restifo NP, Rosenberg SA. Adoptive transfer of syngeneic T cells transduced with a chimeric antigen receptor that recognizes murine CD19 can eradicate lymphoma and normal B cells. Blood. 2010;116:3875–86.
33. Abraham RT, Weiss A. Jurkat T cells and development of the T-cell receptor signalling paradigm. Nat Rev Immunol. 2004;4:301–8.
34. Hope JL, Otero DC, Bae EA, Stairiker CJ, Palete AB, Faso HA, et al. PSGL-1 attenuates early TCR signaling to suppress CD8+ T cell progenitor differentiation and elicit terminal CD8+ T cell exhaustion. Cell Rep. 2023;42:112436.
35. Thatte A, Ficarro S, Snapp KR, Wild MK, Vestweber D, Hunt DF, et al. Binding of function-blocking mAbs to mouse and human P-selectin glycoprotein ligand-1 peptides with and without tyrosine sulfation. J Leukoc Biol. 2002;72:470–7.
36. Pereira JL, Cavaco P, da Silva RC, Pacheco-Leyva I, Mereiter S, Pinto R, et al. P-selectin glycoprotein ligand 1 promotes T cell lymphoma development and dissemination. Transl Oncol. 2021;14:101125.
37. Bezman NA, Jhatakia A, Kearney AY, Brender T, Maurer M, Henning K, et al. PD-1 blockade enhances elotuzumab efficacy in mouse tumor models. Blood Adv. 2017;1:753–65.
38. Davila ML, Kloss CC, Gunset G, Sadelain M. CD19 CAR-targeted T cells induce long-term remission and B cell aplasia in an immunocompetent mouse model of B cell acute lymphoblastic leukemia. PLoS ONE. 2013;8:e61338.
39. Saule P, Trauet J, Dutriez V, Lekeux V, Dessaint JP, Labalette M. Accumulation of memory T cells from childhood to old age: Central and effector memory cells in CD4+ versus effector memory and terminally differentiated memory cells in CD8+ compartment. Mech Ageing Dev. 2006;127:274–81.
40. Pereira JL, Ferreira F, dos Santos NR. Antibody targeting of surface P-selectin glycoprotein ligand 1 leads to lymphoma apoptosis and tumorigenesis inhibition. Hematol Oncol. 2024;42:e3257.

ACKNOWLEDGEMENTS

The authors thank Ivette Pacheco-Leyva and Liliana Oliveira (i3S, Porto) for technical expertise, Mário Sousa Pimenta (IPO-Porto, Porto) for insightful clinical advice, Flávia Pereira (i3S, Porto) for providing healthy donor T cells, Nuno L. Alves for providing reagents, Edwin Hawkins (WEHI, Australia) for providing Eμ-*Myc* cells and members of the Intercellular Communication and Cancer Group (i3S, Porto) for fruitful discussions. The authors acknowledge the support of the Animal Facility, Cell Culture and Genotyping, Translational Cytometry, and Histology and Electron Microscopy (member of the national infrastructure PPBI - Portuguese Platform of Bioimaging; PPBI-POCI-01-0145-FEDER-022122) i3S Scientific Platforms. This work was supported by grants from Gilead Sciences Portugal (*Programa Gilead GÉNESE* ref. no. PGG/038/2017), and *Associação Portuguesa Contra a Leucemia* (APCL) in partnership with Sociedade Portuguesa de Hematologia (SPH) and Gilead Sciences Portugal, by *Fundação para a Ciência e a Tecnologia* (FCT; Portugal), in the framework of the project *Financiamento Plurianual de Unidades de I&D* (UIBD/04293/2020), by *Programa Operacional Regional do Norte by European Regional Development Fund* (ERDF), under the project "The Porto Comprehensive Cancer Center", with the reference NORTE-01-0145-FEDER-072678—Consórcio PORTO.CCC—Porto.Comprehensive Cancer Center, and European Social Fund, and ERDF (NORTE-01-0145-FEDER-000029 and POCI-01-0145-FEDER-007274). JLP was supported by an FCT fellowship (SFRH/BD/147979/2019) and NRS by an FCT CEEC contract (CEECINST/00091/2018/CP1500/CT0020). The graphical abstract was created using BioRender.com.

AUTHOR CONTRIBUTIONS

JLP and NRS designed this research study. JCM, DD, and NRS supervised this study. JLP, LA, AM, RFS, DD, and NRS were involved in designing the experiments. JLP, LA, FF, and AM performed the research. JLP, LA, FF, and NRS analyzed data. JLP, JCM, DD, and NRS interpreted the results. DP provided human lymphoma biopsies. AM and JLP processed the human lymphoma samples. DP, AMC, MJO, JCM, and DD provided multiple reagents. JLP and NRS wrote the manuscript. AMC, MJO, JCM, and DD edited the manuscript. All authors contributed to the preparation of the manuscript and approved the submitted version.

COMPETING INTERESTS

The authors declare no competing interests.

ETHICS APPROVAL AND CONSENT TO PARTICIPATE

Mouse experimental procedures were approved by the i3S ethics committee (approval no. 15/CECRI/2020) and Portuguese authorities (*Direção-Geral de Agricultura e Veterinária*; ref. no. 421/000/000/2021) and followed European and Portuguese guidelines (Directive 2010/63/EU and decree laws no. 113/2013 and 1/2019). Peripheral blood was provided by the São João University Medical Centre blood bank after ethical approval (ref. no. 398/2020). Lymphoma biopsies were obtained at the Onco-Hematology Department of Portuguese Oncology Institute (Porto) after ethical approval (ref. GOM_PI_2013.03). Informed consent was obtained from all participants.

ADDITIONAL INFORMATION

Supplementary information The online version contains supplementary material available at https://doi.org/10.1038/s41375-024-02446-w.

Correspondence and requests for materials should be addressed to Nuno R. dos Santos.